RESEARCH ARTICLE

Programming the nucleation of DNA brick self-assembly with a seeding strand

Yingwei Zhang,* Aleks Reinhardt, Pengfei Wang, Jie Song, Yonggang Ke*

Abstract: The emergence of structural DNA nanotechnology has enabled us to design the self-assembly of nanostructures and nanomachines with nanoscale precision. Recently, DNA brick strategy has provided a highly modular and scalable approach for the construction of complex structures, which can be used as nanoscale pegboards for the precise organization of molecules and nanoparticles for many applications. Despite the dramatic increase of structural complexity provided by DNA brick method, the assembly pathways are still poorly understood. Here, we introduce a "seed" strand to control the crucial nucleation and assembly pathway in DNA brick assembly. Through experimental study and computer simulation, we successfully demonstrate that the regulation of the assembly pathways via seeded growth can accelerate the assembly kinetics and increase the optimal temperature by ~4-7 °C for isothermal assembly. By improving our understanding of the assembly pathways, we provide new guidelines for the design of programmable pathways to improve the self-assembly of DNA nanostructures.

Introduction

Structural DNA nanotechnology provides a powerful molecular self-assembly technique to construct sophisticated nanostructures and nanodevices with great complexity in a controllable and programmable manner.[1] The largest and most complex DNA nanostructures have typically been made using two methods: DNA origami and DNA bricks.[1c, 2] DNA origami, which utilizes a long single-stranded scaffold typically derived from a viral genome with thousands of nucleotides (nt), produces custom-designed one-dimensional (1D), two-dimensional (2D) and three-dimensional (3D) objects by annealing the scaffold via its hybridization with hundreds of short staple strands.[3] By contrast, in the DNA brick strategy, only short building blocks are used to provide a scalable and modular method for fabricating complex structures of arbitrary shapes in both 2D and 3D.[4] These building blocks are short single-stranded DNA molecules, each consisting of four binding domains designed to interlock the bricks to form the target structures. The DNA brick method provides a powerful platform for precise fabrication of functional nanomaterials.[5] Nonetheless, further development of this technology is hindered by an incomplete understanding of the assembly pathways.

Several recent simulation and experimental studies focusing on DNA brick systems provided new insights into the crucial nucleation phase and the following growth stage, as well as on modifying the nucleation barrier by rationally designing the topology of interactions within the target structures.[6] These studies have shown that conventional DNA brick assembly was initiated by a "random" nucleation process where small nuclei consisting of a few DNA bricks located at various positions of the target structure (Figure 1a). The formation of these random nuclei — structurally similar but different in DNA sequences — is a low-frequency event in the microscopic regime, which leads to overall slow assembly in bulk. Thus, initial nucleation of conventional DNA brick assembly is the rate-limiting step in the whole assembly process and determined by the highly nonclassical nucleation barrier, where finite clusters form before the critical cluster size is reached.[7] A subsequent growth phase then produces the complete target structure. We believe it is feasible to program the nucleation process and thus the subsequent assembly pathway to improve the kinetics and thermodynamic behaviors of DNA brick assembly, by introducing a DNA "seed" strand, based on the previous report of seeded growth for DNA tile-based lattices.[8] In this seeded assembly strategy we introduce here, a single-stranded DNA comprising several hundred bases is included in order to trigger rapid and controlled nucleation, leading to subsequent fast growth (Figure 1b). Because the seed strands contain multiple binding domains to hybridize with several DNA bricks, leading to a more favorable interaction energy, nucleation at the seed strand will be much more likely due to a reduced height of the nucleation free-energy barrier (Figure 1c), and at a given temperature, the rate of nucleation at the seed strand will be considerably higher than that of the much shorter DNA bricks. Hence, we anticipate that the controlled nucleation initiated from the long seed strand will dominate the nucleation stage by significantly speeding up the nucleation process by outcompeting the DNA-brick-only nucleation, particularly at relatively higher temperatures. We therefore propose two hypotheses: (1) the range of optimal isothermal assembly temperatures of DNA brick structures in seeded assembly strategy can be extended (Figure 1d) in comparison to the conventional brick assembly strategy since the free-energy barrier to nucleation greatly depends on

[a] Y. Zhang
State Key Laboratory of Chemical Resource Engineering, College of Materials Science and Engineering, Beijing University of Chemical Technology
Beijing, 100082 (China)
E-mail: zhangyw@mail.buct.edu.cn
Prof. A. Reinhardt
Department of Chemistry, University of Cambridge
Cambridge, CB2 1EW (United Kingdom)
Prof. P. Wang,
Institute of Molecular Medicine, Renji Hospital, School of Medicine, Shanghai Jiao Tong University
Shanghai, 200127 (China)
Prof. J. Song
Department of Instrument Science and Engineering, School of Electronic Information and electrical Engineering, Shanghai Jiao Tong University
Shanghai, 200127 (China)
Prof. Y. Ke
Wallace H. Coulter Department of Biomedical Engineering, Georgia Institute of Technology and Emory University, Emory University School of Medicine
Atlanta, Georgia 30322 (United States)
Email: yonggang.ke@emory.edu

Supporting information for this article, including additional references [15] is given via a link at the end of the document.

temperature;[6a] and (2) the formation of the final assembled structures can be significantly accelerated in seeded assembly of DNA bricks (Figure 1e). To test the seeded assembly strategy and verify our hypotheses, four representative DNA brick structures were tested experimentally, and the results were in agreement with computer simulations.

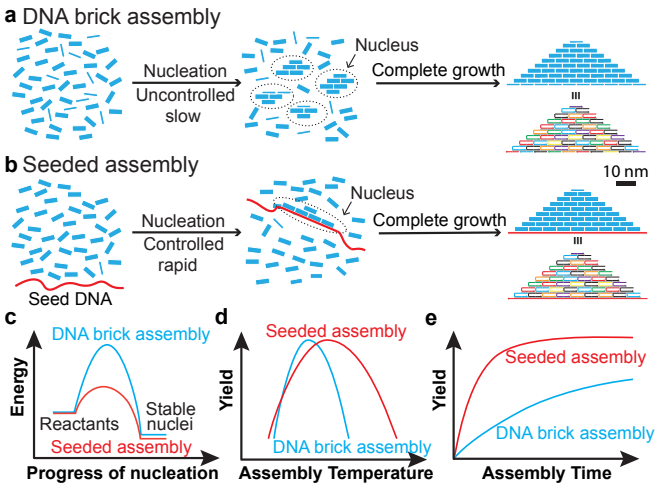

Figure 1. Schematic illustrations comparing conventional DNA brick assembly and the seeded assembly. a) In the DNA brick assembly strategy, the nucleation phase is slow and uncontrolled. b) In the seeded self-assembly strategy, a "seed" strand is used to trigger the rapid and controlled nucleation process and thus accelerate the entire assembly process. c) A schematic illustration of the reduction in energy of the critical nucleus along the nucleation pathway of the seeded strategy. d) and e) our hypotheses: by controlling and accelerating the nucleation, the seeded assembly is expected to initiate assembly at higher temperatures and boost the assembly kinetics.

Results and Discussion

The four representative 2D and 3D DNA brick structures were first designed using the conventional DNA brick method in caDNAno: a small 2D 9H×10T-triangle, a small 2D 9H×10T-rectangle, a large 2D 16H×20T-rectangle, and a large 3D 6H×4H×208B-rod (H: helix; T: tile; B: base pair).[9] Then, to generate the seeded designs, a "seed" strand (P425, comprising 425 nt) was added into these models (Figure S1) to replace the following: (i) 10 brick strands of total length 210 nt on the bottom edge of the small 2D 9H×10T-triangle and 9H×10T-rectangle, (ii) 20 brick strands of total length 420 nt on the bottom edge of the large 2D 16H×20T-rectangle, (iii) 15 brick strands of total length 416 nt on one face of the large 3D 6H×4H×208B-rod. The seed strand contributes 10%, 6.5%, 3.2% and 4.1% mass to the complete small triangle, small rectangle, large rectangle, and large 3D rod, respectively. The sizes of DNA bricks and the target structures are shown in Figure S1. The P425 seed strand was excised from a 7308-nt m13 phage DNA. Methods and protocols for the P425 preparation and the assembly of DNA structures are included in the Supporting information, and details of the magnesium ion concentration used and how it was optimized are shown in Figures S2, S7 and S14 and section S3.1 of the SI.

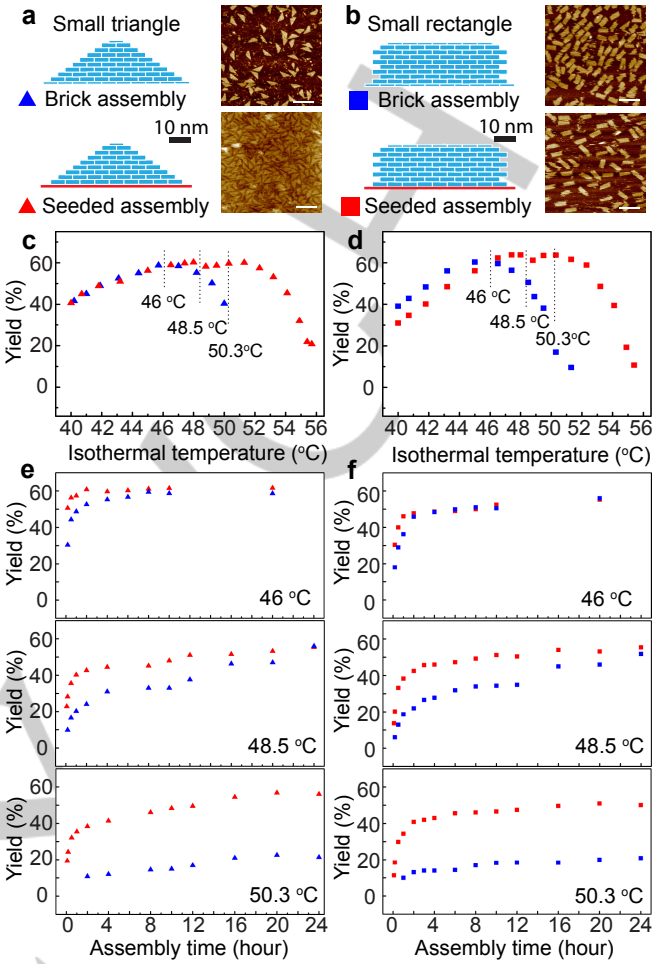

Figure 2. a,b) Schematics and AFM images of the 9H×10T-triangle and the 9H×10T-rectangle. c-d, Product yields after annealing the 2D structures at different temperatures using the 20-hour isothermal annealing protocol. e-f) Assembly kinetics were studied by analyzing product yields over a range of time points from 5 min to 24 hours at three isothermal assembly temperatures: 46 °C, 48.5 °C, 50.3 °C. All the scale bars are 100 nm.

The seeded assembly strategy was firstly tested with the small 9H×10T-triangle and 9H×10T-rectangle by comparing the isothermal assembly temperature and kinetics between the conventional brick assembly strategy and the seeded assembly strategy (Figure 2). The isothermal assembly of the 9H×10T-triangle and 9H×10T-rectangle was performed at temperatures from 40 °C to 56 °C for 20 hours (Figure 2c and 2d). By comparing the product yields from gel electrophoresis assays (details of yield analysis are included in Figure S3, Table S1 and sections S3.3 of the Supporting Information), we found the seeded assembly strategy significantly increased the optimal assembly temperature by ~5 °C for both the triangle and rectangle structures (see details given in Table S1), with the highest assembly temperature approaching 54-55 °C, compared to below 50 °C for the corresponding non-seeded DNA brick products. The successful assembly of the 9H×10T-triangle and 9H×10T-rectangle with expected morphologies was confirmed by AFM imaging on the purified products extracted from the product bands with highest

yields in the agarose gels (Figure 2a and 2b). The different assembly temperature profiles between the brick strategy and the seeded assembly strategy were also observed by monitoring the real-time fluorescence signal variation versus temperature during a thermal annealing process (Figure S4). Therefore, these results strongly suggest that the introduction of the seed strand had broadened and elevated the assembly temperatures for DNA brick structures. To further examine the seeded assembly, especially at the early stages of the assembly, we also studied the assembly kinetics by analyzing the complete product yields at different time points under different isothermal annealing temperatures (Figure 2e and 2f; gel electrophoresis results are included in Figure S5 and S6). We observed the first appearance of the fully assembled products in the seeded assembly at much earlier time points than in the conventional brick strategy, which showed only smearing at the same time points. This further analysis showed that the seeded assembly exhibited accelerated kinetics compared to conventional brick assembly before reaching the equilibrium stages (maximum yields of the target structure).

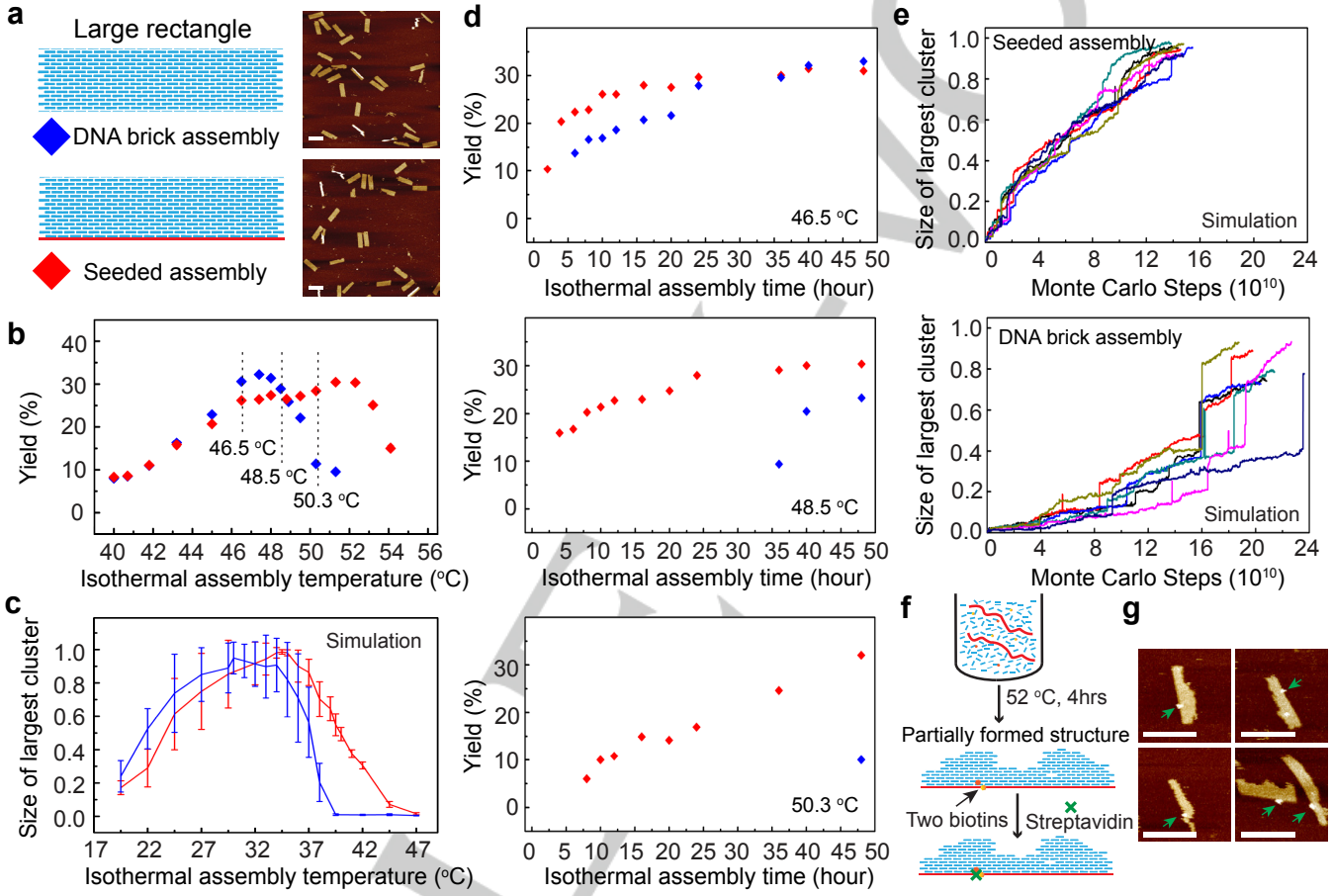

Figure 3. a) Schematics and AFM images of the 16H×20T-rectangle. b) Experimental comparison of the yields of the DNA brick assembly and the seeded assembly using 48-hour isothermal assembly. c) The size of the largest correctly formed clusters from fixed-temperature Monte Carlo simulations as a function of isothermal assembly temperature via two strategies. Each data point represents the average of 10 independent simulations in the long-time limit and error bars show the SD. d) Experimental product yields as a function of isothermal assembly time at 46.5 °C, 48.5 °C and 50.3 °C. e) A comparison of assembly as a function of Monte Carlo time in simulations of seeded and unseeded assembly at 37 °C. Vertical jumps in cluster size correspond to the merging of clusters rather than the addition of individual DNA bricks to the largest cluster in the system. f) Schematic to illustrate the path of nucleation and growth starting from the seed side at 52 °C by using a biotin-streptavidin modification on seed side to label the partially assembled products taken from an initial reaction time of 4 hours. g) AFM images of partially assembled structures from 4 hours at 52 °C using the seeded assembly strategy with arrows highlighting the biotin-streptavidin modification on the seed side. All the scale bars in AFM images are 100 nm.

To test the seeded assembly strategy more thoroughly, we investigated the effects of seed strand in the assembly of the 16H×20T-rectangle, which is about 4 times the size of the small rectangle structure. When comparing the isothermal assembly temperatures, an increase of the optimized temperature of ~4 °C was observed in the seeded assembly strategy compared to the conventional approach (Figure 3b, Figure S8 and Table S1). In thermal annealing experiments, we also observed that seeded assembly produced the rectangle structures at higher temperatures than brick assembly (Figure S9). In order to gain a

more microscopic insight into the self-assembly process, we performed coarse-grained Monte Carlo simulations of this large 2D structure both with and without a seed strand in simulations with a single copy of the target structure. We show in Figure 3c the mean size of the largest cluster in the system as a function of temperature in the limit of long times. Although in single-target simulations, the depletion effect is rather more pronounced than in bulk experiments,[6b] the behavior of these curves mirrors that of Figure 3b, with the largest mean cluster size achieved at a higher temperature for systems in which a seed molecule was present. Seed strands lower the free-energy barrier to nucleation and affect the nucleation behavior itself.[6b, 6c] An analysis of mean first-passage times, assuming all remaining terms in the expression for the rate are unchanged,[6b] shows a reduction of the height of the nucleation free-energy barrier by 2.0 k_BT at 37°C when the seed strand is introduced into the system. These simulations thus support our hypothesis: the spontaneous nucleation process of DNA bricks is slow and involves thermal fluctuations that overcome a temperature-dependent free-energy barrier.[7] At high temperatures, nucleation cannot occur at experimentally reasonable time scales and no product is formed.[6c] By contrast, when the P425 seed is included in the reaction mixture, nucleation involving this strand can occur much more readily at higher temperatures, since the strand has longer continuous complementary sections with its neighbours, which allows for favourable bonding without incurring a significant entropic penalty. Since the strand is connected to many other molecules in the target structure, it can then act as a template for growth, changing the self-assembly pathway.[6a, 6c] The higher the temperature at which assembly can occur, the less likely is the formation of incorrect base-pairs, which can then frustrate the subsequent formation of the target structure.[7] Maximum yields can therefore most readily be achieved if we can shift nucleation to occur at higher temperatures. Although the nucleation free-energy barrier can be overcome at lower temperatures, kinetic aggregates due to incorrect bonding of clusters become increasingly more likely to occur,[6a, 7, 10] leading to a decrease in yields in both strategies as the temperature is decreased (Figure 3c; see Figure S10).

We choose three temperatures, 46.5 °C, 48.5 °C, 50.3 °C, to study the assembly kinetics for the large 2D rectangle structure. Compared with unseeded brick assembly, both the initial and the overall rate of assembly were faster for seeded assembly (Figure 3d; Figure S11). We also use Monte Carlo simulations to investigate the assembly kinetics from monomers for both systems (Figure 3e). At 37 °C, the seeded structure is able to assemble nearly to completion in a considerably shorter time than the unseeded analogue. Although growth is somewhat faster for the seeded structure, the primary reason for this behaviour is that the remainder of the structure grows atop the seed molecule and no lead-in time is required for homogeneous nucleation to occur. By contrast, in the unseeded case, a thermal fluctuation is required to overcome the nucleation free-energy barrier, which limits the rate of self-assembly, as we hypothesised in Figure 1 and b. The faster kinetics of the seeded assembly strongly suggested that the nucleation stage was dominated by the seeded nucleation, and the subsequent growth of DNA bricks should largely follow the pathways guided by the seeds. To validate this conclusion, we investigated the seeded assembly pathways of the 16H×20T-rectangle experimentally at 52 °C. In order to test whether nucleation primarily occurs at the seed molecule, we labelled two bricks – one on and one adjacent to the seed-side edge – with a biotin modification. When hybridized, the two labelled bricks can capture streptavidin, as illustrated in Figure 3f. The products obtained from three representative time points (4 h, 24 h and 48 h) were isolated and then incubated with streptavidin. In order to extract both incomplete and complete structures for subsequent AFM characterization, we ran gel electrophoresis and cut the gel roughly around the target band. We observed that after 4 h almost all the recognizable structures were incomplete with obvious streptavidin-label (Figure 3g), and after 24 h some fully formed structures appeared alongside many streptavidin-labelled incomplete structures. Finally, after 48 h, the majority of products were fully formed structures, and there were only relatively few incomplete structures present (Figure S12a). Of these incomplete structures, 82-88% have a streptavidin label (Figure S12b), and all of them appear to have slender rectangle-like morphologies with missing fragments located on the side opposite that of the seed molecule. Considering the typical successful streptavidin labelling results in a 91-93% success rate (Figure S12b), these findings confirm that nucleation and growth do indeed start at the seed strand at 52 °C when a seed molecule is present. We obtained similar results at 46.5 °C, even though spontaneous nucleation is likely to be thermally accessible at this temperature (Figure S13). Under comparable conditions in simulations, we observe that overwhelmingly, the nucleation pathway begins along the seed strand (Figure S12c), confirming that the seed strand directs the entire self-assembly process by facilitating nucleation.

We further expanded our study on the seeded assembly to the large 3D 6H×4H×208B-rod (Figure 4a). Firstly, the seeded assembly strategy showed an advantage of being able to assemble the rod structure at a relatively lower DNA concentration of 100 nM per strand compared to the 200 nM minimal concentration for the unseeded brick strategy under the same assembly condition (Figure S14), perhaps because the seed strand enables facile nucleation. The experimental assays and simulation analysis on the isothermal assembly also revealed significantly broadened and increased assembly temperatures for the seeded assembly vs the brick assembly (Figure 4b and c; Figure S15, Table S1). The products assembled at their respective optimized temperatures of brick assembly strategy and seeded assembly strategy (26 °C and 33 °C) were imaged by TEM after gel purification and the sizes matched well with the rod design as shown from different lateral projections of the cylindrical model (Figure S16). These experimental findings can again be supported by simulation results, where we can observe that at lower temperatures, clusters tend to bond incorrectly and

aggregate together, since a number of nuclei can form simultaneously when the nucleation free-energy barrier is low. At somewhat higher temperatures, misbonding is less favourable and the nucleation free-energy barrier is sufficiently large to inhibit large-scale nucleation in the unseeded brick system. As a result, nucleation largely only occurs at the seed molecule, and seeded assembly results in a significantly larger number of assembled structures (Figure S17), both when a single target and when multiple targets are simulated (see Figure S18). In both simulation and experiment, seeded assembly leads to significantly faster nucleation kinetics (Figure 4d-g; Figure S18, S19). The advantages of the seeded assembly strategy in both rates of growth and the quality of the resulting product at higher temperatures are thus apparent for this large 3D structure as well.

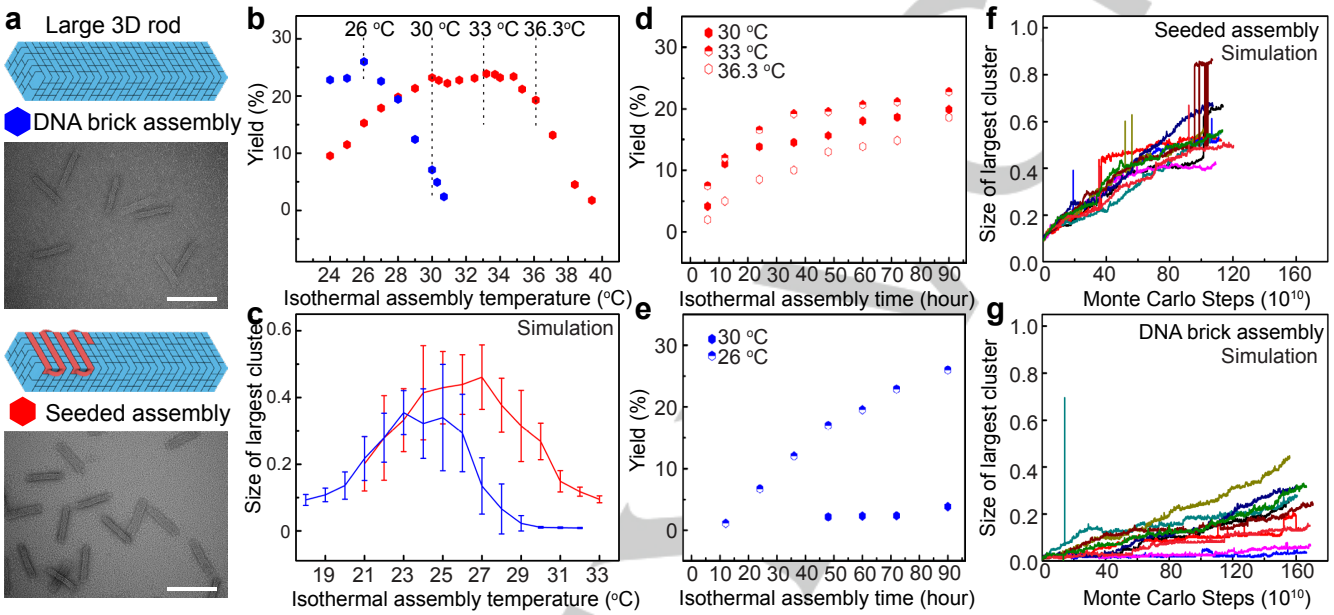

Figure 4. a) Schematics and TEM images of the 6H×4H×208B-rod. Scale bars are 100 nm. b) Experimental comparison of the assembly yields of the DNA brick assembly and the seeded assembly by annealing sample at different temperatures using 90-hour isothermal annealing. c) The size of the largest correctly formed cluster from fixed-temperature Monte Carlo simulations as a function of temperature for both seeded and unseeded systems. Each data point represents the average of 10 independent simulations in the long-time limit and error bars show the SD. d) and e) Experimental product yields as a function of isothermal assembly time at several temperatures. f) and g) A comparison of assembly as a function of Monte Carlo time in multi-target simulations of seeded and unseeded assembly at 27 °C.

Finally, we studied the thermal stability of pre-assembled DNA structures both with and without seed molecules at elevated temperatures. First, large 2D and 3D structures were pre-assembled via the two strategies at their corresponding optimized temperatures and used as a control. After 1-hour incubation at higher temperatures, we determined the residual target-band intensity ratio of these structures as a function of temperature. For the large 2D rectangle structure, the seeded structure begins to melt significantly at temperatures higher than those of the unseeded structure in both experiment and Monte Carlo simulation (Figure S20a to c), indicating that the seed strand provides a stronger protection for the structure, probably due to the decreased nick points (which weaken the base stacking interactions in the case of brick strategy) in its located helix, which may provide a kinetic barrier to the disassembly.[1m, 2b, 6b, 11] Unlike in the assembly process, the disassembly of pre-assembled structures appears to start at the opposite end of the structure, i.e. the one not protected by the seed strand (Figure S20d),[6b, 6c] while unseeded structures can disassemble from all sides simultaneously, speeding up the disassembly kinetics. This speculation is confirmed by simulation snapshots (inset of Figure S20b). For the 3D rod structure, there is a negligible difference in the disassembly behavior between the seeded and unseeded structures (Figure S21). Since the seed strand occupies only part of a single boundary face, its protective function is weaker than in the 2D structure, and so its effect on the kinetics of disassembly is reduced. Locally, the seed molecule's interaction with its immediate neighbors are still favourable (Figure S21d, inset), so the disassembly of the immediate neighbours only takes place at higher temperatures on thermodynamic grounds. Hence, it seems that the designed location of this seed strand in the seeded assembly strategy plays a key role in maintaining the stability of the corresponding local structure and should be carefully considered in future structure designs.

Conclusion

Nucleation is the first and perhaps the most important step in the DNA self-assembly process or protein polymerization.[12] The "seeded" assembly strategy we have proposed significantly affects the nucleation behavior even though only a small portion of the target structure is altered. We have demonstrated experimentally and using computer simulations that the addition of a long seed strand controls the kinetics of structure assembly. The seed strand leads to a reduced height of the nucleation free-energy barrier, which in turn results in a broadened temperature range of successful self-assembly and a higher overall temperature at which self-assembly can occur. Such a higher assembly temperature reduces the propensity for incorrect assembly, which becomes a significant problem as the temperature is decreased; the larger the temperature gap between these regimes, the more successful the self-assembly process is like to be. Moreover, the location of the seed strand can affect the stability of the target structure: molecules at the outer faces of target structures are less likely to attach to the growing structure because their reduced connectivity reduces the energetic favourability of bonding, but the seed strand, with longer regions of complementarity between neighbours, helps to counter this effect. As a result, structures can form more fully at higher temperatures, and furthermore, they are less prone to disassembly as the system is heated. The proposed seeded assembly strategy provides a preferred assembly pathway starting from rapid nucleation at the seed strand outwards, leading to a greatly reduced assembly time compared to the conventional brick assembly strategy which usually requires long assembly times of dozens of hours or several days.[2b, 4, 13]

By investigating the behavior of seeded assembly in detail, we have gained a deeper understanding for the assembly process of DNA brick structures and improved our ability to manipulate and control DNA brick systems. In future, we can potentially engineer more complex behaviors of DNA brick assembly. For instance, it is possible to introduce multiple seed strands in a DNA brick assembly. These seed strands can be purposefully designed to induce nuclei at different temperatures, which would allow us to control the assembly products by using different temperature profiles for the assembly. The multiple seed strands can also be programmed to produce different nuclei, leading to the formation of multiple controlled products in a single assembly process. Moreover, such an understanding will allow us to design rationally both complex and large DNA structures in the future with higher thermodynamic stability and rapid assembly rates, which is of particular importance in enabling further precise modifications of other functional species at the molecular scale to be made for many possible attractive applications. Considering the benefits brought about by DNA seed strand, we believe this improved strategy for DNA brick structure assembly may be particularly advantageous for the higher-level hierarchical assembly of DNA structures or the fabrication of dynamically transformable structures requiring structure units with superior complexity and thermal stability.[1j, 3b, 14]

Acknowledgements ((optional))

Y. Zhang thanks the support from Natural Science Foundation of China (grants 51672022, 51302010). Y. Ke acknowledges NSF grants DMR-1654485 and ECCS-1807568, and Semiconductor Research Corporation (SRC) grant 2836.002. A. Reinhardt acknowledges resources provided by the Cambridge Research Computing Service funded by EPSRC Tier-2 capital grant EP/P020259/1. The AFM images were collected on an AFM supported by grants GM084070 and 3R01GM084070-07S1 to Laura Finzi. All data underpinning this research are included in the article and its supporting information.

Keywords: DNA nanotechnology• DNA brick• Self-assembly• seeded assembly• controlled nucleation

[1] a) N. C. Seeman, *Nature* **2003**, *421*, 427-431; b) W. M. Shih, J. D. Quispe, G. F. Joyce, *Nature* **2004**, *427*, 618-621; c) P. W. Rothemund, *Nature* **2006**, *440*, 297-302; d) S. M. Douglas, H. Dietz, T. Liedl, B. Hogberg, F. Graf, W. M. Shih, *Nature* **2009**, *459*, 414-418; e) J. Zheng, J. J. Birktoft, Y. Chen, T. Wang, R. Sha, P. E. Constantinou, S. L. Ginell, C. Mao, N. C. Seeman, *Nature* **2009**, *461*, 74-77; f) D. Han, S. Pal, J. Nangreave, Z. Deng, Y. Liu, H. Yan, *Science* **2011**, *332*, 342-346; g) R. Iinuma, Y. Ke, R. Jungmann, T. Schlichthaerle, J. B. Woehrstein, P. Yin, *Science* **2014**, *344*, 65-69; h) A. N. Marchi, I. Saaem, B. N. Vogen, S. Brown, T. H. LaBean, *Nano. Lett.* **2014**, *14*, 5740-5747; i) E. Benson, A. Mohammed, J. Gardell, S. Masich, E. Czeizler, P. Orponen, B. Hogberg, *Nature* **2015**, *523*, 441-444; j) T. Gerling, K. F. Wagenbauer, A. M. Neuner, H. Dietz, *Science* **2015**, *347*, 1446-1452; k) R. Veneziano, S. Ratanalert, K. Zhang, F. Zhang, H. Yan, W. Chiu, M. Bathe, *Science* **2016**, *352*, 1534; l) J. Li, A. A. Green, H. Yan, C. Fan, *Nat. Chem.* **2017**, *9*, 1056-1067; m) J. Song, Z. Li, P. Wang, T. Meyer, C. Mao, Y. Ke, *Science* **2017**, *357*; n) P. Wang, T. A. Meyer, V. Pan, P. K. Dutta, Y. Ke, *Chem* **2017**, *2*, 359-382; o) N. Liu, T. Liedl, *Chem. Rev.* **2018**, *118*, 3032-3053; p) K. Huang, D. Yang, Z. Tan, S. Chen, Y. Xiang, Y. Mi, C. Mao, B. Wei, *Angew. Chem. Int. Ed.* **2019**, *58*, 12123-12127.

[2] a) B. Wei, M. Dai, P. Yin, *Nature* **2012**, *485*, 623-626; b) Y. Ke, L. L. Ong, W. M. Shih, P. Yin, *Science* **2012**, *338*, 1177-1183; c) P. Yin, R. F. Hariadi, S. Sahu, H. M. T. Choi, S. H. Park, T. H. LaBean, J. H. Reif, *Science* **2008**, *321*, 824-826.

[3] a) F. Hong, F. Zhang, Y. Liu, H. Yan, *Chem. Rev.* **2017**, *117*, 12584-12640; b) G. Tikhomirov, P. Petersen, L. Qian, *Nature* **2017**, *552*, 67-71; c) K. F. Wagenbauer, C. Sigl, H. Dietz, *Nature* **2017**, *552*, 78; d) S. M. Douglas, J. J. Chou, W. M. Shih, *Proc. Natl. Acad. Sci. U. S. A.* **2007**, *104*, 6644-6648.

[4] L. L. Ong, N. Hanikel, O. K. Yaghi, C. Grun, M. T. Strauss, P. Bron, J. Lai-Kee-Him, F. Schueder, B. Wang, P. Wang, J. Y. Kishi, C. Myhrvold, A. Zhu, R. Jungmann, G. Bellot, Y. Ke, P. Yin, *Nature* **2017**, *552*, 72.

[5] B. L. Cannon, D. L. Kellis, P. H. Davis, J. Lee, W. Kuang, W. L. Hughes, E. Graugnard, B. Yurke, W. B. Knowlton, *ACS Photonics* **2015**, *2*, 398-404.

[6] a) W. M. Jacobs, A. Reinhardt, D. Frenkel, *Proceedings of the National Academy of Sciences* **2015**, *112*, 6313-6318; b) H. K. Wayment-Steele, D. Frenkel, A. Reinhardt, *Soft Matter* **2017**, *13*, 1670-1680; c) M. Sajfutdinow, W. M. Jacobs, A. Reinhardt, C. Schneider, D. M. Smith, *Proc. Natl. Acad. Sci. U. S. A.* **2018**, *115*, E5877-E5886; d) L. Cademartiri, K. J. Bishop, *Nature materials* **2015**, *14*, 2-9; e) W. M. Jacobs, D. Frenkel, *J. Am. Chem. Soc.* **2016**, *138*, 2457-2467; f) P. Fonseca, F. Romano, J. S. Schreck, T. E. Ouldridge, J. P. K. Doye, A. A. Louis, *J. Chem. Phys.* **2018**, *148*, 134910.

[7] A. Reinhardt, D. Frenkel, *Phys. Rev. Lett.* **2014**, *112*, 238103.

[8] a) A. M. Mohammed, R. Schulman, *Nano. Lett.***2013**, *13*, 4006-4013; b) D. Woods, D. Doty, C. Myhrvold, J. Hui, F. Zhou, P. Yin, E. Winfree, *Nature* **2019**, *567*, 366-372.

[9] S. M. Douglas, A. H. Marblestone, S. Teerapittayanon, A. Vazquez, G. M. Church, W. M. Shih, *Nucleic Acids Res.* **2009**, *37*, 5001-5006.

[10] W. M. Jacobs, A. Reinhardt, D. Frenkel, *J. Chem. Phys.* **2015**, *142*, 021101.

[11] P. Yakovchuk, E. Protozanova, M. D. Frank-Kamenetskii, *Nucleic Acids Res.* **2006**, *34*, 564-574.

[12] a) R. Schulman, E. Winfree, *Proc. Natl. Acad. Sci. U. S. A.* **2007**, *104*, 15236-15241; b) Y. Yamakita, F. Oosawa, S. Yamashiro, F. Matsumura, *J. Biol. Chem.* **2003**, *278*, 17937–17944.

[13] Y. Ke, L. L. Ong, W. Sun, J. Song, M. Dong, W. M. Shih, P. Yin, *Nat. Chem.* **2014**, *6*, 994-1002.

[14] a) A. Rajendran, M. Endo, Y. Katsuda, K. Hidaka, H. Sugiyama, *ACS Nano* **2011**, *5*, 665-671; b) E. Kopperger, J. List, S. Madhira, F. Rothfischer, D. C. Lamb, F. C. Simmel, *Science* **2018**, *359*, 296-301; c) S. Li, Q. Jiang, S. Liu, Y. Zhang, Y. Tian, C. Song, J. Wang, Y. Zou, G. J. Anderson, J.-Y. Han, Y. Chang, Y. Liu, C. Zhang, L. Chen, G. Zhou, G. Nie, H. Yan, B. Ding, Y. Zhao, *Nat. Biotechnol.* **2018**, *36*, 258.

[15] a) P. Wang, M. A. Rahman, Z. Zhao, K. Weiss, C. Zhang, Z. Chen, S. J. Hurwitz, Z. G. Chen, D. M. Shin, Y. Ke, *J. Am. Chem. Soc.* **2018**, *140*, 2478-2484; b) A. Reinhardt, C. P. Ho, D. Frenkel, *Faraday Discuss.* **2016**, *186*, 215-228; c) S. Whitelam, P. L. Geissler, *J. Chem. Phys.* **2007**, *127*, 154101; d) J. John SantaLucia, D. Hicks, *Annu. Rev. Biophys. Biomol. Struct.* **2004**, *33*, 415-440.

Entry for the Table of Contents (Please choose one layout)

Layout 1:

RESEARCH ARTICLE

Through experimental study and computer simulation, a “seeded-assembly” strategy was developed to control the crucial nucleation and assembly pathway in DNA brick assembly by accelerating the assembly kinetics, lowing the free-energy barrier to nucleation and increasing the optimal temperatures for isothermal assembly.

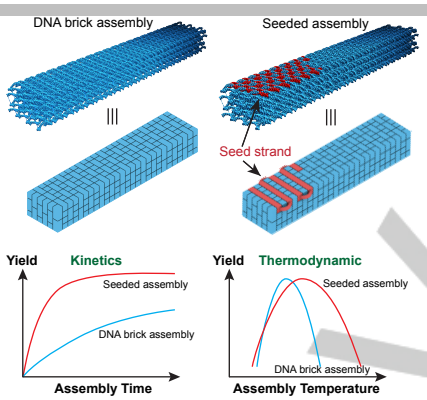

Yingwei Zhang, Aleks Reinhardt, Pengfei Wang, Jie Song, Yonggang Ke**

Page No. – Page No.

Programming the nucleation of DNA brick self-assembly with a seeding strand